

# Confocal laser scanning microscopy and optical coherence tomography for the evaluation of the kinetics and quantification of wound healing after fractional laser therapy

Elke Christina Erika Sattler, MD,<sup>a</sup> Katharina Poloczek,<sup>b</sup> Raphaela Kästle,<sup>b</sup> and Julia Welzel, MD, PhD<sup>b</sup>  
*Munich and Augsburg, Germany*

**R**esurfacing techniques are well-established methods for skin rejuvenation, treatment of acne scars, wrinkles, or melasma. Ablative techniques are highly effective, but bear the risk of persisting pigmentation, infection, or scarring.<sup>1-3</sup> To reduce such side effects and to achieve faster completion of wound healing, the so-called “sub-surfacing” by means of nonablative techniques was introduced, which causes controlled dermal

#### *Abbreviations used:*

CLSM: confocal laser scanning microscopy  
DEJ: dermoepidermal junction  
MAZ: microscopic ablation zone  
OCT: optical coherence tomography

hyperthermia sparing the integrity of the epidermis.<sup>4-6</sup>

---

From the Departments of Dermatology and Allergology at Ludwig-Maximilian University of Munich<sup>a</sup> and General Hospital Augsburg.<sup>b</sup>

The first two authors contributed equally to this article.

Funding sources: None.

Conflicts of interest: None declared.

Accepted for publication April 26, 2013.

Reprint requests: Julia Welzel, MD, PhD, Department of Dermatology and Allergology, General Hospital Augsburg,

---

Sauerbruchstraße 6, 86179 Augsburg, Germany. E-mail: [julia.welzel@klinikum-augsburg.de](mailto:julia.welzel@klinikum-augsburg.de).

In 2004 the new concept of fractional photothermolysis was formed. This technique creates microscopically small thermal denatured tissue columns, so-called “microscopic treatment zones,” with a high number of focused laser beams. This way only about 10% to 20% of the skin is treated while the surrounding tissue is spared.<sup>7-9</sup> The microscopic treatment zones are replaced by new collagen within 3 to 6 months.<sup>9,10</sup>

The ablative variant of fractional photothermolysis evolved in 2007. The erbium: yttrium-aluminum-garnet laser (2940 nm) or the carbon-dioxide laser (10,600 nm) cause microscopic ablation zones (MAZ) due to the strong absorption of water. The MAZ is covered by a crust and surrounded by a coagulation zone with denatured collagen, bordering a hyperthermia zone. Heat shock proteins are released and re-epithelization is performed within 48 hours.<sup>11</sup> Crucial for the postfractional

wound healing is the percentage of treated skin, meaning the density of the MAZ.<sup>12-14</sup> The long-term effect of neocollagenesis and the stimulation of the production of hyaluronic acid take about 1 to 3 months.<sup>12,13</sup>

So far all this information was gathered by histopathological and immunohistochemical examinations, which always implied the need for an invasive biopsy and—once taken—the same area of skin could not be assessed over time.

Confocal laser scanning microscopy (CLSM) and optical coherence tomography (OCT) offer noninvasive visualization of the superficial layers of the skin in vivo in real time. Although CLSM allows very detailed imaging with almost histopathological resolution of the epidermis and papillary dermis with a limited penetration depth of about 250  $\mu\text{m}$ , OCT has a lower resolution of about 3 to 7  $\mu\text{m}$ , but gives insights down to about 1.7 mm deep. CLSM is meanwhile established as a diagnostic tool for the diagnosis of melanoma and nonmelanoma skin cancers,<sup>15-25</sup> but also for a wide range of other skin diseases.<sup>26-33</sup> OCT also has a variety of indications, but is mainly used for the diagnosis and treatment monitoring of nonmelanoma skin cancer.<sup>32,34-38</sup> Because of their noninvasiveness, a big advantage of both techniques is the possibility of evaluating the

same site of skin over time—ideal for monitoring of dynamic processes such as wound healing.

The aim of this study was to determine whether CLSM and OCT can be used to observe and quantify the kinetics of the dynamic process of wound healing and to evaluate the effects of fractional laser therapy noninvasively in the period right after treatment until up to 21 days posttreatment.

## CAPSULE SUMMARY

- The effects of fractional laser therapy have thus far been studied mainly using histologic examination. Recently, long-term effects have been examined using confocal laser scanning microscopy.
- Confocal laser scanning microscopy and optical coherence tomography enable the visualization of wound healing after fractional laser therapy at the same site over time within the first 3 weeks posttreatment.
- The possibility to study wound healing in vivo over time will improve the understanding of the therapeutic effects of fractional laser treatment.

## METHODS

### Probands

With approval of the ethical committee of our university, 20 healthy volunteers were recruited after written informed consent. Included were only adults between 18 and 65 years of age with healthy skin on the future test areas.

The study was conducted between October 2010 and February 2011 in the Department of Dermatology, General Hospital Augsburg, Germany.

### Study performance

All probands received a standardized application of fractional ablative laser treatment using a carbon-dioxide laser (QuadraLASE, Candela Laser Deutschland GmbH, Neu-Isenburg, Germany) with a wavelength of 10,600 nm. A precise scanning matrix of microspots in a lattice pattern can be produced. The following parameters were used: optical spot size 300  $\mu\text{m}$ , field square-shaped 7  $\times$  7 mm, pulse duration 3.5 milliseconds, coverage 10%, and laser power 8 and 16 W, respectively. This led to 48 MAZ per test field.

The previously untreated test areas were placed on the proximal third of the volar forearm 2 cm apart from each other. Probands were numbered consecutively and the first 10 panelists received 8 W in the proximal test field and 16 W in the distal area, whereas in probands 11 through 20, the laser power was applied vice versa.

### Measurements

Measurements were performed at 6 different time points: before the laser treatment (T0), right after laser application (T1), and on day 1 (T2), day 3 (T3), day 7 (T4), day 14 (T5), and day 21 (T6). Using a confocal laser microscope (VivaScope 1500 Multiwave, Mavig, Munich, Germany), a mosaic of 5  $\times$  5 mm within each test field was scanned

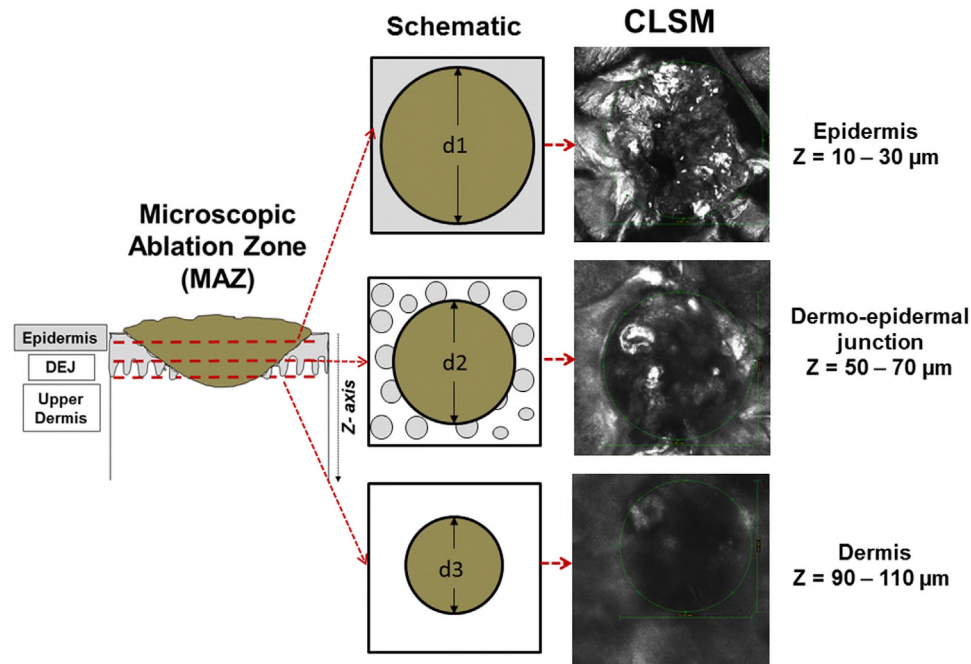


**Fig 1.** Schematic diagram of microscopic ablation zone (MAZ) with horizontal sectional images and corresponding confocal images. *CLSM*, Confocal laser scanning microscopy; *DEJ*, dermoepidermal junction.

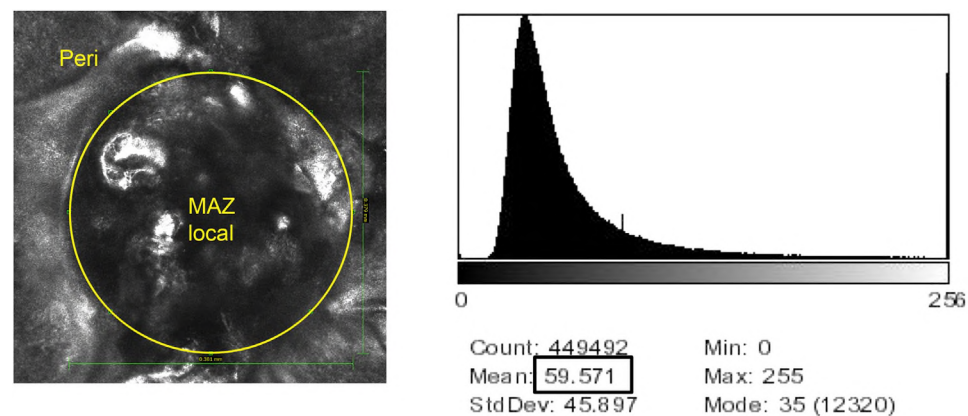


**Fig 2.** Confocal image of microscopic ablation zone (MAZ) (left) and histogram of gray values of selected area (right).

horizontally in 3 depths: epidermis, dermoepidermal junction (DEJ), and papillary dermis. In addition, a profile into the depth of 2 MAZ per test area was performed, using the VivaStack function with 10- $\mu\text{m}$  steps downward to a depth of 200  $\mu\text{m}$ . Measurement of the MAZ diameter was obtained by using the circle tool of the software program VivaScan (Mavig, Munich, Germany). For standardization purposes, the measurements were performed on the VivaStack (Mavig, Munich, Germany) images: for the epidermis ( $z = 10\text{--}30 \mu\text{m}$ ), for the DEJ ( $z = 50\text{--}70 \mu\text{m}$ ), and for the dermis ( $z = 90\text{--}100 \mu\text{m}$ ) (Fig 1). Next, the signal

intensities were evaluated in the same images of  $500 \times 500 \mu\text{m}$  using the software Image J to measure the brightness of the pixel per area with possible scores between 0 and 256. Using the histogram function, the signal intensity of the entire confocal image (“peri”) was measured and then compared with the signal intensity measured within the MAZ (“loc”) (Fig 2).

At the same time points, images were taken with the frequency domain OCT system Callisto (Thorlabs AG, Lübeck, Germany), which works at 930 nm. It offers a lateral scan length of 4 mm, a depth penetration of about 1.7 mm, and an axial resolution of 7  $\mu\text{m}$ .

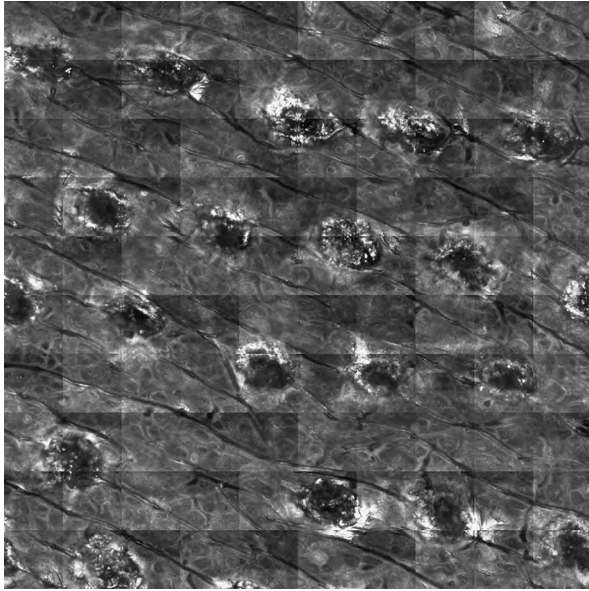


**Fig 3.** Confocal image right after laser treatment. Microscopic ablation zones are easily distinguishable as dark areas of denaturation without definable cell structures (VivaBlock mosaic [Mavig, Munich, Germany], 5 × 5 mm; z = 40 μm).

### Statistical analysis

Statistical calculations were performed using software (SPSS 19, IBM Corp, Armonk, NY). For the analysis of the data between the different time points and for intraindividual comparisons of the 2 test sites, the Wilcoxon pair test for connected probes was used. *P* value less than .05 was rated as statistically significant.

### RESULTS

Of the 20 healthy volunteers, aged 22 to 60 years (median 50.5), 5 were male and 15 were female.

#### Morphologic changes over time

Clinically, erythema and edema could be seen in all test areas right after laser treatment (T1), being more pronounced in the areas treated with the higher laser power. Up to day 3 (T3) all MAZ wounds were covered with little crusts. These were starting to fall off around day 7 (T4), significantly earlier in the 16-W areas than in the 8-W areas. By day 21 (T6), all crusts had fallen off and, clinically, wound healing was completed superficially.

#### Changes visualized by CLSM

In correlation, CLSM imaging showed the following morphologic changes at the 6 different time points at the 3 different levels (epidermis, DEJ, dermis):

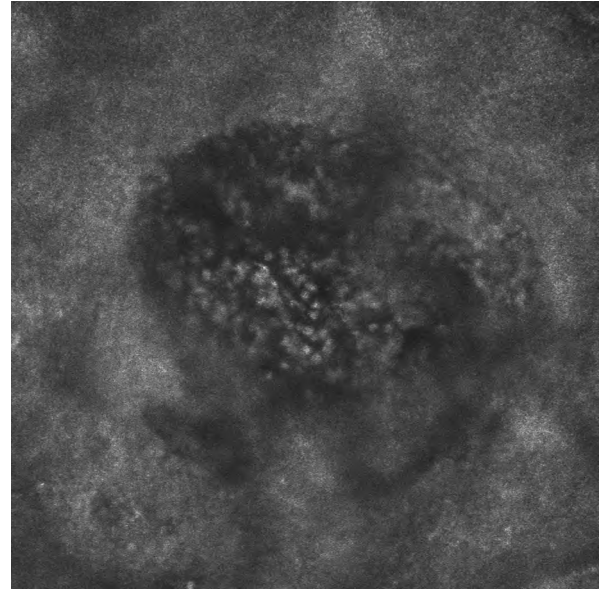


**Fig 4.** Confocal image on day 1 after laser treatment, showing inflammatory phase, with small round, bright cells in field of microdefect and its surrounding (single confocal image, 500 × 500 μm, z = 80 μm).

At T1, MAZ are clearly distinguishable as dark areas of denaturation caused by thermal necrosis without definable cell structures within (Fig 3).

At T2, small round, bright cells demonstrate the beginning of the inflammatory phase (Fig 4).

On the level of the epidermis, an amorphous, crusty plaque has formed at T3 (Fig 5, A), whereas on the level of the DEJ the first reformation of honeycomb pattern—typical for the normal epidermal pattern seen in CLSM—can be seen indicating the beginning of re-epithelization (Fig 5, B). On the level of the dermis, low refractile, subepidermal damage is visible (Fig 5, C).

At T5, re-epithelization is completed: the newly formed epidermis impresses with higher refractility than the surrounding spared tissue (Fig 6, A), whereas at the DEJ, the MAZ still appear as well-demarcated, low refractile areas with a brighter center (Fig 6, B) and in the dermis the MAZ still show the lower refractile substance defects (Fig 6, C).

After 21 days (T6), subepidermal damage is still visible in 89.5% of test areas treated with a laser power of 8 W and in all areas treated with 16-W laser power (Fig 7).

#### Diameter of MAZ over time visualized by CLSM

The diameter of the MAZ was greatest at T1 right after treatment with a mean of 385 μm at 8-W laser power and with 422-μm diameter at 16 W. The

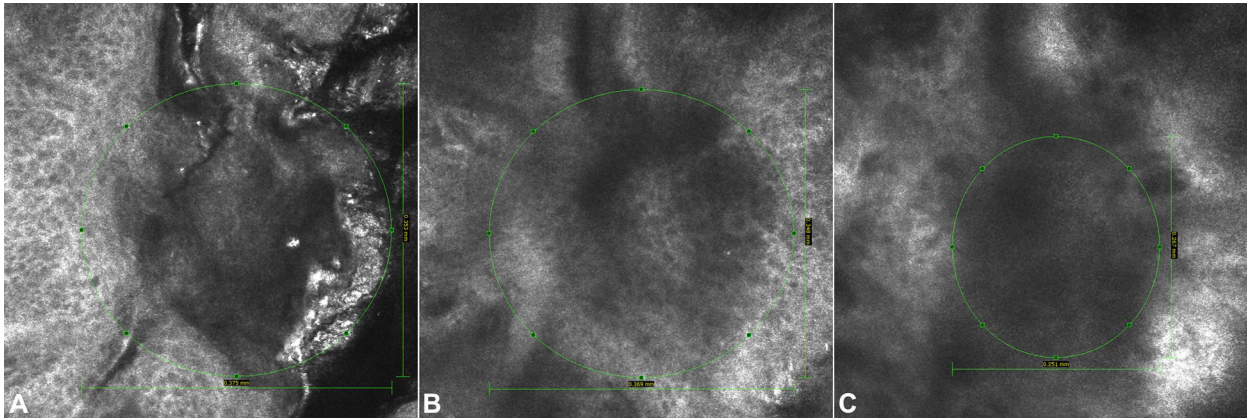


**Fig 5.** Confocal images of same microscopic ablation zone at 3 different levels on day 3 after laser treatment. **A**, Epidermis: amorphous, crusty plaque. **B**, Dermoepidermal junction: beginning re-epithelization with early reestablishment of honeycomb pattern. **C**, Dermis: low refractile, subepidermal damage.

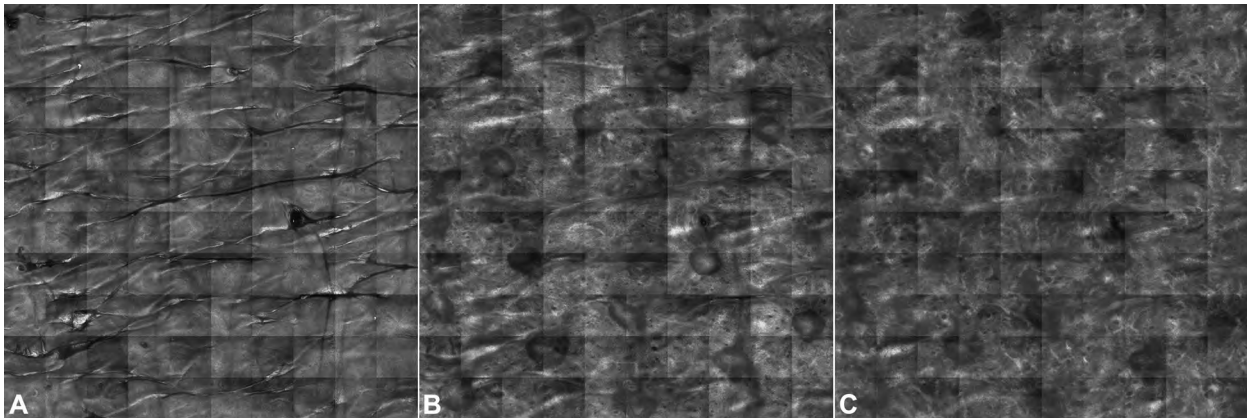


**Fig 6.** Confocal mosaics of 1 microscopic ablation zone (MAZ) at 3 different levels on day 14 after laser treatment. **A**, Epidermis: re-epithelization completed. **B**, Dermoepidermal junction: MAZ appear as well-demarcated, low refractile areas with brighter center. **C**, Dermis: lower refractile substance defects.

measurement of the diameter of the MAZ shows a continuous reduction on all 3 levels over time. Because of a quick cockle of the wound edges within the first 24 hours, the reduction of diameter of the MAZ in the epidermis is significantly smaller from T1 to T2. Up to day 3 (T3), the diameter of the wounds created with 16 W is significantly bigger than the ones produced with 8 W. On the level of the DEJ and in the dermis, the reduction of diameter is similar. Even on day 21 an ablation zone is still remarkable on both deeper levels. The effect of the higher laser power is clearly visible, with significantly higher values at all time points for the 16 W-treated areas. Especially on day 21 (T6) a faster wound healing presented by faster reduction in diameter of the defects is noticeable (Fig 8).

#### Local signal intensity of MAZ over time visualized by CLSM

In all 3 levels, a significant decrease in signal intensity is seen directly after laser treatment, with the greatest in the dermis. In accordance with the faster epidermal normalization clinically, the continuous increase of signal intensity after T1 to T6 is quicker in the epidermal level and takes longest to return toward normal in the dermis, without reaching the original starting values (T0 = untreated skin) by day 21 (Fig 9).

#### Depth of MAZ over time visualized by OCT

The deep skin defects caused by the ablation can be seen in the OCT image as dark structureless areas (Fig 10).

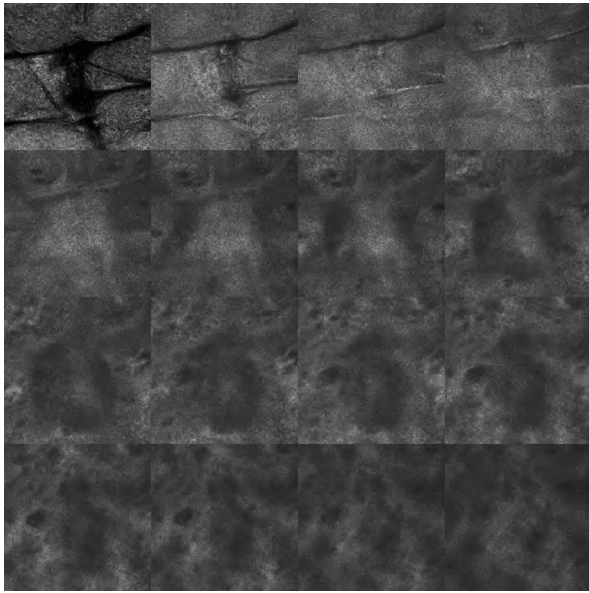


**Fig 7.** VivaStack at day 21 after laser treatment, demonstrating that subepidermal damage is still visible 3 weeks after treatment (from *left to right*, z-range from 10-160  $\mu\text{m}$  with z-depth of 10  $\mu\text{m}$  between images).

The maximal depths of the MAZ reached into the papillary dermis with a maximum of 184  $\mu\text{m}$  at 8-W laser power on T4 and of 227  $\mu\text{m}$  at 16-W laser power on T3 (Table I).

Exemplary histology of a lesion directly after fractional therapy with the QuadraLASE (Candela Laser Deutschland GmbH) (power 8 W) is demonstrated in Fig 11 and correlates well with the OCT images. In this single histologic correlate, the depth of the MAZ reaches 240  $\mu\text{m}$ .

## DISCUSSION

Fractional laser therapy has become a standard procedure for skin resurfacing in aesthetic dermatology. In this randomized controlled study 20 healthy volunteers were treated with a fractional carbon-dioxide laser that produces standardized skin defects in form of MAZ. By using CLSM and OCT as imaging tools, we were able to visualize and quantify the kinetics of the wound-healing process and the therapeutic effects in the upper layers of the skin in real time. In addition to the detection of superficial morphologic changes (inflammation, crusts), CLSM also enables a look in almost histopathological resolution at the level of the DEJ and the papillary dermis, whereas OCT is even able to image down to about 1.7 mm, yet with a lower resolution. In the majority of treated areas, the subepidermal defects were still detectable even after 21 days. Measurement of the diameter of the MAZ over time quantified the much faster course of wound healing

at the epidermal level compared with the deeper layers, which is the aim of fractional laser treatment. This differs from our general understanding of wound healing as we know it from ulcers or other chronic wounds, where we are used to a “bottom-up healing process” concept. The CLSM findings were also sustained by the decrease and recovery times of the signal intensity within the MAZ, which were greater and took longer to return toward normal in the deeper layers.

Correlation of the specific characteristics seen by CLSM and OCT to the findings known from histopathological studies was excellent; MAZ are displayed as typical cone-shaped lesions with superficial necrotic debris. Already after 1 day with the induction of the inflammatory phase of wound healing, a diffuse infiltration with inflammatory cells is seen within and around the MAZ, probably featuring neutrophils, as demonstrated in molecular studies.<sup>39</sup> On day 3, crusts cover the surface. CLSM shows a newly formed honeycomb pattern below, representing re-epithelization. Heat shock proteins are thought to play an important role in the fast replacement of the keratinocytes, especially heat shock protein 70.<sup>11,40</sup> Also the induction of growth factors and proinflammatory cytokines enables the fast progression of wound healing.<sup>41-43</sup> In another histologic study, a granulomatous inflammation reaction in the dermis could still be seen 4 weeks after treatment with a laser power of 300 mJ.<sup>44</sup> This corresponds well to the long-lasting zones of dermal defect described in our study and supports the recommendation to allow an interval of at least 4 weeks between treatments for the completion of the ongoing remodeling process and to avoid scarring.<sup>44</sup> Results by Longo et al<sup>45</sup> on the long-term effects (3-12 weeks) of fractional laser therapy analyzed by CLSM complement ideally our results of the short-term effects. They could confirm that the collagen seen before treatment was replaced by a new collagen type showing an intense collagen remodeling, which was still visible 3 months posttreatment demonstrating the long-term effect of laser treatment.

The depth of the ablation zone measured by OCT reached into the papillary dermis. This is similar to representative histology right after a laser shot with the same laser. The depth increased within the first days after laser treatment with a maximum after 3 to 7 days. This effect might be caused by a contraction of the heated collagen directly after the treatment and/or to further necrosis of the coagulated collagen a few days after treatment. Yet in histologic studies a surrounding coagulation zone is described leading to the long-lasting remodeling effect.<sup>13</sup> Evaluation and quantification of the degree of the collagen

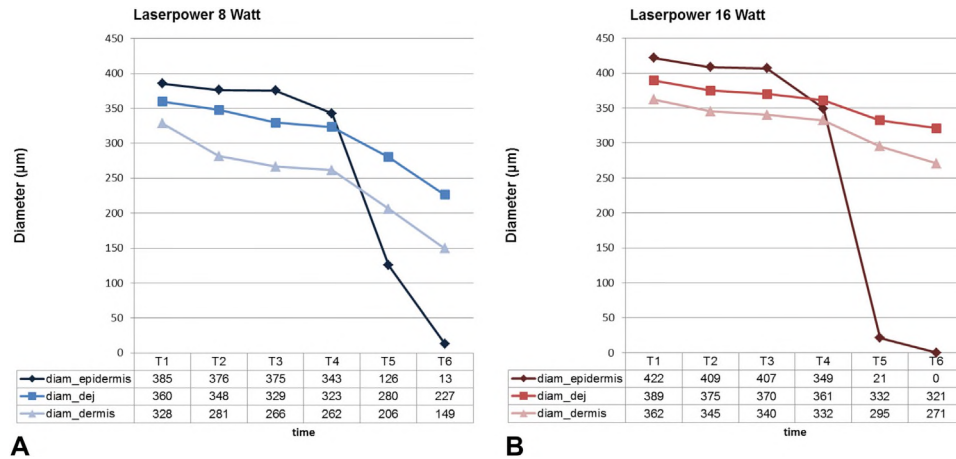


**Fig 8.** Decrease of diameter of microscopic ablation zones over time. Test areas treated with 8 W (A) and 16 W (B). *Dej*, Dermoepidermal junction; *T1*, right after laser treatment; *T2*, after 1 day; *T3*, after 3 days; *T4*, after 7 days; *T5*, after 14 days; *T6*, after 21 days.

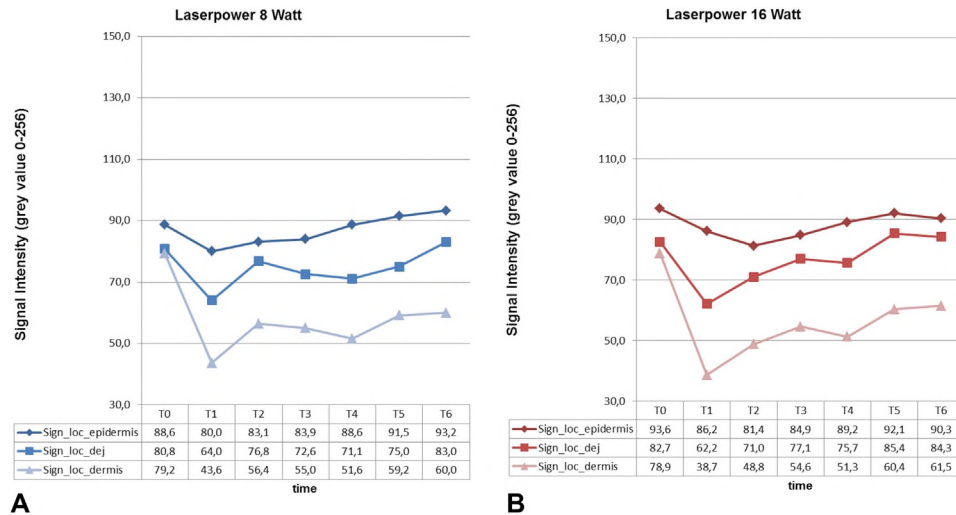


**Fig 9.** Course of local signal intensity of microscopic ablation zones over time. Test areas treated with 8 W (A) and 16 W (B). *Dej*, Dermoepidermal junction; *T1*, right after laser treatment; *T2*, after 1 day; *T3*, after 3 days; *T4*, after 7 days; *T5*, after 14 days; *T6*, after 21 days.

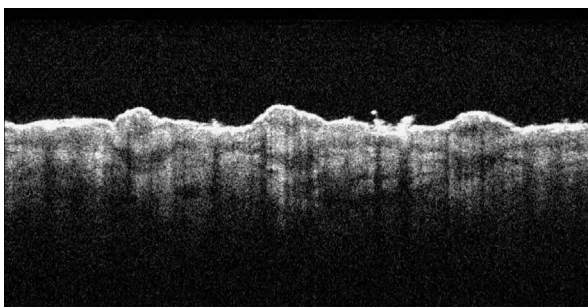


**Fig 10.** Optical coherence tomography image after 7 days with laser power of 16 W. Dark structureless areas correspond to microscopic ablation zones.

denaturation around the ablation zones using OCT have been described in several studies.<sup>46,47</sup>

In this study, measurements were performed at 6 time points over a 21-day observation period. Usually the phases of wound healing are supposed to take a maximum of 3 to 4 weeks for completion. Other experimental studies, which also tried to evaluate the benefit of CLSM or OCT for the monitoring of wound healing, chose an observation period of 12 or even only 8 days.<sup>48,49</sup> Although the period of 21 days chosen here was helpful to evaluate the acute healing process, it was too short to monitor the entire collagen remodeling process. Details on these long-term effects of laser treatment were recently evaluated by CLSM and described, supporting the thesis that the dermal remodeling process really takes several months, as suggested formerly by the long-lasting expression of heat shock proteins.<sup>13,45</sup>

**Table I.** Optical coherence tomography measurements of depths of microscopic ablation zones ( $\mu\text{m}$ ) over time

Laser power	T1	T2	T3	T4	T5	T6
8 W	91 $\pm$ 9	157 $\pm$ 25*	182 $\pm$ 17*	184 $\pm$ 17	157 $\pm$ 24*	143 $\pm$ 16 <sup>†</sup>
16 W	128 $\pm$ 12	200 $\pm$ 24*	227 $\pm$ 21*	224 $\pm$ 18	192 $\pm$ 21*	189 $\pm$ 18 <sup>†</sup>

Significant change of value compared with one before within same test field calculated by Wilcoxon test: <sup>†</sup> $P \leq .05$ , \* $P \leq .01$ .

Mean values  $\pm$  SD.

T1, Right after laser treatment; T2, after 1 day; T3, after 3 days; T4, after 7 days; T5, after 14 days; T6, after 21 days.

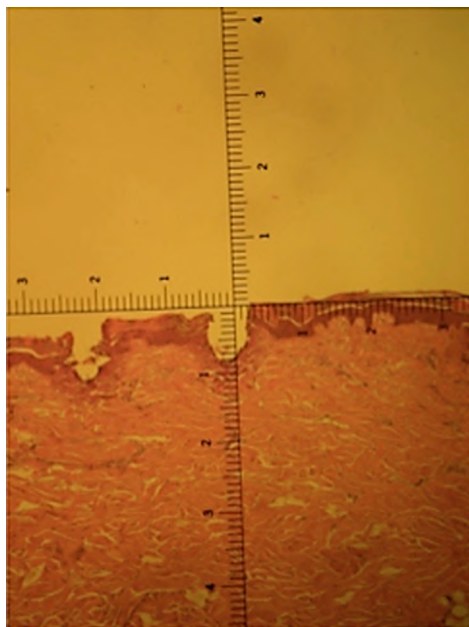


**Fig 11.** Exemplary histology of lesion directly after fractional therapy with QuadraLASE (Candela Laser Deutschland GmbH, Neu-Isenburg, Germany) (laser power 8 W) demonstrating good correlation with optical coherence tomography image shown in Fig 10. In this single histologic correlate, depth of microscopic ablation zone reaches 240  $\mu\text{m}$ .

In summary, CLSM and OCT enable us to monitor changes noninvasively, and thus to observe the effects of laser therapy of the same unaltered site over time without repetitive biopsies. The results of our study may serve as a basis for comparison in patients with complications after laser treatment such as infection or prolonged wound healing.

#### REFERENCES

- Bernstein LJ, Kauvar AN, Grossman MC, Geronemus RG. The short- and long-term side effects of carbon dioxide laser resurfacing. *Dermatol Surg* 1997;23:519-25.
- Manuskiatti W, Fitzpatrick RE, Goldman MP. Long-term effectiveness and side effects of carbon dioxide laser resurfacing for photoaged facial skin. *J Am Acad Dermatol* 1999;40:401-11.
- Manuskiatti W, Siriphukpong S, Varothai S, Wanitphakdeedecha R, Fitzpatrick RE. Effect of pulse width of a variable square pulse (VSP) erbium:YAG laser on the treatment outcome of periorbital wrinkles in Asians. *Int J Dermatol* 2010;49:200-6.
- Alexiades-Armenakas MR, Dover JS, Arndt KA. The spectrum of laser skin resurfacing: nonablative, fractional, and ablative laser resurfacing. *J Am Acad Dermatol* 2008;58:719-37; quiz 38-40.
- Bernstein EF, Ferreira M, Anderson D. A pilot investigation to subjectively measure treatment effect and side-effect profile of non-ablative skin remodeling using a 532 nm, 2 ms pulse-duration laser. *J Cosmet Laser Ther* 2001;3:137-41.
- Zelickson BD, Kilmer SL, Bernstein E, Chotzen VA, Dock J, Mehregan D, et al. Pulsed dye laser therapy for sun damaged skin. *Lasers Surg Med* 1999;25:229-36.
- Manstein D, Herron GS, Sink RK, Tanner H, Anderson RR. Fractional photothermolysis: a new concept for cutaneous remodeling using microscopic patterns of thermal injury. *Lasers Surg Med* 2004;34:426-38.
- Bedi VP, Chan KF, Sink RK, Hantash BM, Herron GS, Rahman Z, et al. The effects of pulse energy variations on the dimensions of microscopic thermal treatment zones in nonablative fractional resurfacing. *Lasers Surg Med* 2007;39:145-55.
- Laubach HJ, Manstein D. Fractional photothermolysis [in German]. *Hautarzt* 2007;58:216-8, 20-3.
- Laubach HJ, Tannous Z, Anderson RR, Manstein D. Skin responses to fractional photothermolysis. *Lasers Surg Med* 2006;38:142-9.
- Helbig D, Moebius A, Simon JC, Paasch U. Nonablative skin rejuvenation devices and the role of heat shock protein 70: results of a human skin explant model. *J Biomed Opt* 2010;15:038002.
- Bogdan Allemann I, Kaufman J. Fractional photothermolysis—an update. *Lasers Med Sci* 2010;25:137-44.
- Hantash BM, Bedi VP, Kapadia B, Rahman Z, Jiang K, Tanner H, et al. In vivo histological evaluation of a novel ablative fractional resurfacing device. *Lasers Surg Med* 2007;39:96-107.
- Grunewald S, Bodendorf MO, Simon JC, Paasch U. Update dermatologic laser therapy. *J Dtsch Dermatol Ges* 2011;9:146-59.
- Gonzalez S. Confocal reflectance microscopy in dermatology: promise and reality of non-invasive diagnosis and monitoring. *Actas Dermosifiliogr* 2009;100(Suppl):59-69.
- Gonzalez S, Swindells K, Rajadhyaksha M, Torres A. Changing paradigms in dermatology: confocal microscopy in clinical and surgical dermatology. *Clin Dermatol* 2003;21:359-69.
- Pellacani G, Longo C, Malveyh J, Puig S, Carrera C, Segura S, et al. In vivo confocal microscopic and histopathologic correlations of dermoscopic features in 202 melanocytic lesions. *Arch Dermatol* 2008;144:1597-608.
- Pellacani G, Scope A, Ferrari B, Pupelli G, Bassoli S, Longo C, et al. New insights into nevogenesis: in vivo characterization and follow-up of melanocytic nevi by reflectance confocal microscopy. *J Am Acad Dermatol* 2009;61:1001-13.
- Rajadhyaksha M, Gonzalez S, Zavislan JM, Anderson RR, Webb RH. In vivo confocal scanning laser microscopy of human skin II: advances in instrumentation and comparison with histology. *J Invest Dermatol* 1999;113:293-303.



20. Rajadhyaksha M, Menaker G, Flotte T, Dwyer PJ, Gonzalez S. Confocal examination of nonmelanoma cancers in thick skin excisions to potentially guide Mohs micrographic surgery without frozen histopathology. *J Invest Dermatol* 2001;117:1137-43.
21. Selkin B, Rajadhyaksha M, Gonzalez S, Langley RG. In vivo confocal microscopy in dermatology. *Dermatol Clin* 2001;19:369-77, ix-x.
22. Ulrich M, Gonzalez S, Lange-Asschenfeldt B, Roewert-Huber J, Sterry W, Stockfleth E, et al. Non-invasive diagnosis and monitoring of actinic cheilitis with reflectance confocal microscopy. *J Eur Acad Dermatol Venereol* 2011;25:276-84.
23. Ulrich M, Krueger-Corcoran D, Roewert-Huber J, Sterry W, Stockfleth E, Astner S. Reflectance confocal microscopy for noninvasive monitoring of therapy and detection of subclinical actinic keratoses. *Dermatology* 2010;220:15-24.
24. Ulrich M, Maltusch A, Rius-Diaz F, Rowert-Huber J, Gonzalez S, Sterry W, et al. Clinical applicability of in vivo reflectance confocal microscopy for the diagnosis of actinic keratoses. *Dermatol Surg* 2008;34:610-9.
25. Ulrich M, Maltusch A, Rowert-Huber J, Gonzalez S, Sterry W, Stockfleth E, et al. Actinic keratoses: non-invasive diagnosis for field cancerization. *Br J Dermatol* 2007;156(Suppl):13-7.
26. Astner S, Gonzalez S, Cuevas J, Rowert-Huber J, Sterry W, Stockfleth E, et al. Preliminary evaluation of benign vascular lesions using in vivo reflectance confocal microscopy. *Dermatol Surg* 2010;36:1099-110.
27. Gonzalez S, Gilaberte-Calzada Y. In vivo reflectance-mode confocal microscopy in clinical dermatology and cosmetology. *Int J Cosmet Sci* 2008;30:1-17.
28. Gonzalez S, Rajadhyaksha M, Rubinstein G, Anderson RR. Characterization of psoriasis in vivo by reflectance confocal microscopy. *J Med* 1999;30:337-56.
29. Astner S, Gonzalez S, Gonzalez E. Noninvasive evaluation of allergic and irritant contact dermatitis by in vivo reflectance confocal microscopy. *Dermatitis* 2006;17:182-91.
30. Astner S, Ulrich M. Confocal laser scanning microscopy [in German]. *Hautarzt* 2010;61:421-8.
31. Rothmund G, Sattler EC, Kaestle R, Fischer C, Haas CJ, Starz H, et al. Confocal laser scanning microscopy as a new valuable tool in the diagnosis of onychomycosis—comparison of six diagnostic methods. *Mycoses* 2013;56:47-55.
32. Sattler E, Kaestle R, Rothmund G, Welzel J. Confocal laser scanning microscopy, optical coherence tomography and transonychia water loss for in vivo investigation of nails. *Br J Dermatol* 2012;166:740-6.
33. Sattler E, Kastle R, Arens-Corell M, Welzel J. How long does protection last? In vivo fluorescence confocal laser scanning imaging for the evaluation of the kinetics of a topically applied lotion in an everyday setting. *Skin Res Technol* 2012;18:370-7.
34. Mogensen M, Thrane L, Jorgensen TM, Andersen PE, Jemec GB. OCT imaging of skin cancer and other dermatological diseases. *J Biophotonics* 2009;2:442-51.
35. Ulrich M, Stockfleth E, Roewert-Huber J, Astner S. Noninvasive diagnostic tools for nonmelanoma skin cancer. *Br J Dermatol* 2007;157(Suppl):56-8.
36. Welzel J. Optical coherence tomography in dermatology: a review. *Skin Res Technol* 2001;7:1-9.
37. Welzel J, Lankenau E, Birngruber R, Engelhardt R. Optical coherence tomography of the human skin. *J Am Acad Dermatol* 1997;37:958-63.
38. Sattler E, Kastle R, Welzel J. Optical coherence tomography in dermatology. *J Biomed Opt* 2013;18:061224.
39. Orringer JS, Rittie L, Baker D, Voorhees JJ, Fisher G. Molecular mechanisms of nonablative fractionated laser resurfacing. *Br J Dermatol* 2010;163:757-68.
40. Helbig D, Bodendorf MO, Grunewald S, Kendler M, Simon JC, Paasch U. Immunohistochemical investigation of wound healing in response to fractional photothermolysis. *J Biomed Opt* 2009;14:064044.
41. Asea A, Kraeft SK, Kurt-Jones EA, Stevenson MA, Chen LB, Finberg RW, et al. HSP70 stimulates cytokine production through a CD14-dependant pathway, demonstrating its dual role as a chaperone and cytokine. *Nat Med* 2000;6:435-42.
42. Starnes AM, Jou PC, Molitoris JK, Lam M, Baron ED, Garcia-Zuazaga J. Acute effects of fractional laser on photo-aged skin. *Dermatol Surg* 2012;38:51-7.
43. Werner S, Grose R. Regulation of wound healing by growth factors and cytokines. *Physiol Rev* 2003;83:835-70.
44. Grunewald S, Bodendorf M, Illes M, Kendler M, Simon JC, Paasch U. In vivo wound healing and dermal matrix remodeling in response to fractional CO(2) laser intervention: clinicopathological correlation in non-facial skin. *Int J Hyperthermia* 2011;27:811-8.
45. Longo C, Galimberti M, De Pace B, Pellacani G, Bencini PL. Laser skin rejuvenation: epidermal changes and collagen remodeling evaluated by in vivo confocal microscopy. *Lasers Med Sci* 2013;28:769-76.
46. Pierce MC, Sheridan RL, Hyle Park B, Cense B, de Boer JF. Collagen denaturation can be quantified in burned human skin using polarization-sensitive optical coherence tomography. *Burns* 2004;30:511-7.
47. Oh JT, Lee SW, Kim YS, Suhr KB, Kim BM. Quantification of the wound healing using polarization-sensitive optical coherence tomography. *J Biomed Opt* 2006;11:041124.
48. Cobb MJ, Chen Y, Underwood RA, Usui ML, Olerud J, Li X. Noninvasive assessment of cutaneous wound healing using ultrahigh-resolution optical coherence tomography. *J Biomed Opt* 2006;11:064002.
49. Lange-Asschenfeldt B, Alborova A, Krueger-Corcoran D, Patzelt A, Richter H, Sterry W, et al. Effects of a topically applied wound ointment on epidermal wound healing studied by in vivo fluorescence laser scanning microscopy analysis. *J Biomed Opt* 2009;14:054001.